



Free Vibration Analysis of Rotating Functionally Graded Material Beams on Elastic Foundations Using the Homotopy Perturbation Method

Hayder H. Khaleel^{1*}, Ziadoon M.R. Al-Hadrayi²

¹ Engineering Technical College, Najaf, Al-Furat Al-Awsat Technical University, Al-Najaf 31001, Iraq

² Mechanical Engineering Department, Faculty of Engineering, University of Kufa, Najaf 54001, Iraq

Corresponding Author Email: hayderhashim@atu.edu.iq

Copyright: ©2025 The authors. This article is published by IIETA and is licensed under the CC BY 4.0 license (<http://creativecommons.org/licenses/by/4.0/>).

<https://doi.org/10.18280/mmep.120818>

ABSTRACT

Received: 23 May 2025

Revised: 29 July 2025

Accepted: 8 August 2025

Available online: 31 August 2025

Keywords:

Homotopy Perturbation Method (HPM), Functionally Graded Material (FGM), rotating beams, elastic foundation, free vibration analysis, dimensionless natural frequencies, centrifugal stiffening, boundary conditions

This study addresses free vibration analysis of rotating Functionally Graded Material (FGM) beams lying on elastic foundations using the Homotopy Perturbation Method (HPM). The HPM, a semi-analytical technique combining Homotopy from topology with perturbation methods to solve complex nonlinear equations, is employed to solve the resulting nonlinear eigenvalue problem. Its key advantages include effectively handling system inhomogeneity and nonlinearity while yielding insightful semi-analytical expressions. The resulting governing equations, based on Euler-Bernoulli beam theory and Hamilton's principle, are nondimensionalized to capture centrifugal stiffening, foundation interaction, and material gradation. The HPM is used to solve the obtained nonlinear eigenvalue problem, and the dimensionless natural frequencies and mode shapes are obtained for clamped-clamped (C-C), clamped-simply supported (C-S), and clamped-free (C-F) boundary conditions. Validation against Finite Element Method (FEM) and Lagrange-based solutions confirms the high accuracy of HPM, with relative errors consistently less than 2%. Parametric studies show that dimensionless natural frequencies increase as η and λ increase, whereas the increase of the gradient index of FGM (n) leads to lower frequency values due to the severity degradation (ceramic to metal control). Importantly, C-C boundaries display a 4–5 times higher frequency than C-F configurations, emphasizing boundaries as key limiting factors for design. This study fills a significant void in rotating FGM beam dynamics and demonstrates HPM's capability for complex systems, providing valuable semi-analytical tools for engineering design applications such as turbine blades, robotic arms, and rotating machines in extreme environments.

1. INTRODUCTION

Functionally Graded Materials (FGMs) are an advanced class of composites characterized by continuous material property variation in space and are therefore well-suited for application in aerospace fields, rotational machinery, and high-temperature environments [1]. Functionally graded beams used in turbine blades and robot arms are subject to complex load conditions that include both centrifugally applied loads and an interaction with an elastic foundation [2]. Such conditions result in nonlinear vibration behavior and thus necessitate sound analytical approaches with the capability to accurately predict dynamic performance. Analysis of rotary beams is further complicated because of their sensitivity to centrifugal stiffening and intercoupling of axial and transverse vibrations. Furthermore, the addition of an elastic foundation further complicates the dynamic behavior of the system. Perturbation approaches tend to be inadequate due to their sensitivity to small parameters and thus necessitate exploring alternative approaches, including application of the Homotopy Perturbation Method (HPM). HPM overcomes the shortcomings with linearization and discretization and thus

offers an excellent framework for solving strongly linear as well as strongly nonlinear governing equations typical in rotary FGM beams [3, 4].

One semi-analytical tool is the HPM that mixes classic perturbative methods with homotopic topological ideas. There are conventional perturbation techniques where the coefficient is damped, whereas using HPM, a Homotopy is constructed with an auxiliary parameter which quickly tends to a solution approximation without the need for linearization or discretization. This feature endows HPM with an efficiency for solving nonlinear problems. HPM, as compared to most numerical methods, such as Finite Element Method (FEM), through which it omits long matrix manipulations and presents closed solutions, becomes of more interest to parametric studies on dynamic behavior and analytical insight.

While earlier research on FGM structures has been limited mostly to plates and shells subjected to thermal and mechanical loadings, for example, study [5] applied a three-dimensional asymptotic theory to the vibration analysis of harmonic vibrations of FGM plates, and presented the dynamic response of initially stressed FGM plates subjected to impulsive loadings [6-8]. While these studies give

fundamental insight, rotating FGM beams on elastic foundations are not treated very thoroughly. Research [9] on rotating structures has focused on centrifugal effects on vibration response, which investigated nonlinear axisymmetric vibrations of circular FGM plates and illustrated the effectiveness of semi-analytical solutions. Murali and Raju [10] presented an exhaustive review of the vibration analysis of FGM beams emphasizing why it is important to study their dynamic behavior under various boundary conditions. Ait Atmane et al. [11] studied the free vibration of exponentially graded FGM beams with non-uniform cross-sections, deriving analytical solutions for clamped-free, simple supported, and clamped-clamped boundary conditions. Their work shed light on the frequency characteristics of FGM beams. HPM has gained popularity in solving nonlinear vibration problems. Gao et al. [12] utilized HPM to study the surface acoustic waves in FGM plates, demonstrating its versatility. He [13] put HPM on firm ground as an effective technique for nonlinear differential equations so that solutions could be obtained without making restrictive assumptions. One of the recent contributions by reference [14] used HPM and Schauder's fixed-point theorem to provide periodic solutions for Duffing-type systems, demonstrating its worth for complicated dynamics. Allahverdzadeh et al. [15] investigated nonlinear vibration of thin rectangular functionally graded plates by the HPM. The Duffing-type equation was derived based on von Kármán's dynamic plate theory, and HPM solution was verified by numerical solution comparisons. Moreover, the conditions for periodic oscillatory motion were determined through fixed-point theorem, and the effect of material gradation and geometry parameters on the system's dynamic response was illustrated.

Some studies on the vibration behavior of FGM beams utilized a set of theoretical models to analyze their dynamic behavior. Pradhan and Chakraverty [16] for instance, investigated the influence of various shear deformation models on the free vibration behavior of FGM beams with a focus on their higher-order precision in modeling transverse shearing actions. Through their results, they indicated significant differences in natural frequencies depending on the chosen deformation model, especially in beams with a smooth gradation in material properties.

Centrifugal stiffening, elastic foundation interaction and mixed boundary conditions have been ignored in the previous studies. This is an important limitation since, in practical applications such as that of the turbine blades and robotic arms, these two effects are realized simultaneously and affect the natural frequencies and mode shapes to a large extent. In the other side, the references [15, 16] are partly similar to the present problem in the fact that they assume linearized relations to the elastic coefficients; particularly to the best of our knowledge, these are only by perturbation approaches attempting to study the stability of the stationary solutions assuming in some sense nonlinear couplings, many of them are based on strictly numerical approaches or strictly on classical perturbation and usually with require extensive computations for certain problems and in other cases fail to keep accounted of nonlinear coupling effects in rotating FGM beams.

Similarly, Şimşek [17] carried out a study of fundamental frequencies for FGM beams based on a number of higher-order formulations with an emphasis on material distribution and boundary condition dependencies of fundamental frequencies. Although these earlier studies have contributed to an improved understanding of FGM beam dynamics, most

focused on static cases or on non-rotating conditions and ignored rotation as well as interaction with an elastic foundation—the factors that play a crucial part in applications involving turbine blades as well as those involving machine tool manufacture.

The literature study indicates significant advancement in vibration analyses on FGM beams, plates, and shells. However, there remain noteworthy critical shortcomings. While significant studies have been conducted regarding vibrations in statically or non-rotating FGM beams, dynamic properties in rotating FGM beams mounted on flexible mounts remain insufficiently studied. The rotational-induced effects and their coupled phenomenon involving centrifugal stiffening and coupled axial and transverse vibrations result in added intricacy that is inadequately treated in existing research. Furthermore, interrelation between rotating FGM beams and flexible mounts is insufficiently studied despite its significant implications towards mode forms and frequencies through modal parameters in applications involving turbine blades and field machines. Perturbative approaches generally rely on small parameters and linear approximations that do not capture effectively the nonlinear dynamics associated with spinning FGM beams. Additionally, while studies involving Differential Transform Method (DTM) and FEM have been used to solve acoustic issues raised in beams built from materials involving FGMs, use of the HPM application in a context involving rotating FGM beams mounted on flexible mounts is inadequately researched. There is an urgent need for comparative studies that discuss respective approaches, especially in terms of their accuracy and computationally efficiency. Lastly, a lack of sufficient understanding exists in how gradation indices and boundary conditions affect frequencies associated with beams made up of materials involving FGMs due to insufficient exploration of their implications, leading to an ineffective understanding of how gradation and boundary conditions affect spinning structures.

The main aim of the current study is to study the free vibration behavior of rotating FGM beams resting on elastic foundations using the HPM. The specific objectives consist in obtaining the governing differential equation pertaining to the free vibrations of such rotating FGM beams on an elastic foundation using Euler-Bernoulli beam theory and Hamilton's principle; application of HPM to solve the dimensionless governing equation in order to establish an accurate and effective semi-analytical solution for the system's natural frequencies and mode forms; and comparison of results achieved using HPM with analytical results achieved through the Lagrange method and with numerical results calculated using the FEM in order to validate results from HPM. Additionally, this study aims to investigate how variations in the FGM gradient exponent, dimensionless rotational speed, and dimensionless stiffness of an elastic foundation affect the system's natural frequencies for a rotating FGM beam and to study the implications of different boundary conditions (i.e., clamped-clamped (C-C), clamped-simply supported (C-S), and clamped-free (C-F)) on system vibrational behavior.

The method employed in this research is explained as follows: First, according to Euler-Bernoulli beam theory and Hamilton's principle, a governing equation for the phenomenon of free vibration in an elastic foundation-supported rotating FGM beam is to be formulated and then expressed in a dimensionless form through normalization. The HPM is then to be applied by constructing a Homotopy equation that reduces a given nonlinear problem to an

arrangement of linear sub-problems, which is to be solved iteratively to obtain an approximate solution for dimensionless frequencies as well as mode shapes. Results attained using HPM are to be confirmed using a comparison with results solved using Lagrange and FEM, thus proving accuracy and convergence for results developed using HPM. Additionally, parametric analysis is to be carried out to determine the influence of an FGM material's gradient index, dimensionless rotational speed, and dimensionless stiffness of an elastic foundation on dimensionless frequencies in a rotating FGM beam as well as on competing boundary conditions' influence. Lastly, results are to be compared and discussed about in relation to existing research efforts as they pertain to understanding rotating FGM beams on an elastic foundation and proposing recommendations for future research efforts.

The novelty of the present study lies in its unified analytical framework that simultaneously considers (i) the rotational speed-induced centrifugal stiffening effect, (ii) the influence of elastic foundation stiffness, and (iii) various practically relevant boundary conditions (C-C, C-S, and C-F). Unlike previous research that treated these factors separately or neglected some of them, the present work applies HPM to derive accurate semi-analytical solutions, validates them against Lagrange and FEM results, and quantifies the relative error, thereby ensuring reliability. This comprehensive approach fills a critical gap in the literature and provides valuable insights for designing and optimizing rotating FGM structures.

This study used a method that takes into account as a gap in the literature by providing an elaborate study of free vibration properties of rotating FGM beams resting on elastic foundations. The study proposes using the HPM, which is a highly effective and accurate method for solving highly nonlinear governing equations for rotating FGM beams. In addition, it compares and contrasts HPM with the Lagrange method and the FEM, as well as examines the effects of critical parameters and boundary conditions on the natural frequencies for rotating FGM beams. By filling these gaps, this study contributes considerably to the literature in the domain of structural dynamics and presents valuable insights that find application in the analysis and design of rotating FGM beams in engineering applications.

2. GOVERNING DIFFERENTIAL EQUATIONS AND NONDIMENSIONALIZATION OF PARAMETERS

Consider a rotating FGM beam of rectangular cross-section, positioned on an elastic foundation and rotating synchronously with the foundation, as illustrated in the Figure 1. A Cartesian coordinate system is adopted, where the x -axis aligns with the beam's longitudinal (axial) direction, and the z -axis corresponds to the transverse (thickness) direction. The system rotates about the y -axis at a constant angular velocity Ω . The beam has length L , height h , and width b , while the elastic foundation is characterized by its Winkler elastic foundation K . The beam exhibits a continuous material gradation along its thickness (z -axis), transitioning from a fully ceramic upper surface ($z=h/2$) to a fully metallic lower surface ($z=-h/2$). Material properties, including elastic modulus E , Poisson's ratio ν , and mass density ρ , vary as smooth functions of the thickness coordinate z . These graded properties are governed by a power-law distribution based on the rule of mixtures, expressed as [18-24]:

$$P(z) = P_c \left(\frac{z + \frac{h}{2}}{h} \right)^n + P_m \left[1 - \left(\frac{z + \frac{h}{2}}{h} \right)^n \right] \quad (1)$$

where, P_c and P_m denote the material properties of the ceramic and metal constituents, respectively, and n represents the volume fraction exponent governing the gradation profile.

Eq. (1) represents the properties of the ceramic and metallic constituents, respectively, and n is the gradient index. The power-law distribution used to describe the material properties of the functionally graded beam guarantees a smooth variation of properties like density and Young's modulus through the thickness. How quickly the material changes through the thickness are determined by the gradient index n . A fully ceramic beam with maximum stiffness and minimum density is produced by $n=0$, whereas a fully metallic beam with lower stiffness and generally greater ductility is produced by $n \rightarrow \infty$. Intermediate values of n result in smooth property gradations and enable customized stiffness-to-weight ratios.

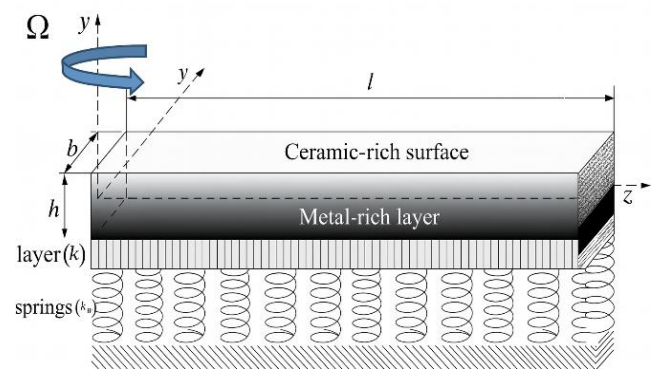


Figure 1. Schematic configuration and coordinate system of a dynamically rotating functionally graded beam resting on a Winkler-type elastic foundation [23]

The governing equations of the rotating FG beam result from an application of Hamilton's principle, which provides an association of strain energy U , kinetic energy T , and work done by external forces W , within the dynamics of the system. The variational formulation of dynamic equilibrium is obtained by minimizing the action integral from time t_1 to t_2 [24].

$$\delta \int_{t_1}^{t_2} (T - U + W) dt = 0 \quad (2)$$

where, δ is the variational operator, and t_1 and t_2 are the initial and final times of motion, respectively.

Let $u(x, t)$ and $w(x, t)$ denote axial and transverse displacements, respectively, of a point on the neutral axis of the beam. Following Euler-Bernoulli beam theory, displacement at any (x, z) in the cross-section is expressed as:

$$u_x(x, t) = u(x, t) - z \frac{\partial w(x, t)}{\partial x}, \quad u_z(x, t) = w(x, t) \quad (3)$$

The strain energy consists of contributions related to bending deformation, centrifugal stiffening, and to the Winkler foundation's elasticity:

$$U = \frac{1}{2} \int_0^l \left[A_1 \left[\frac{\partial u}{\partial x} \right]^2 - 2B_1 \frac{\partial u}{\partial x} * \frac{\partial^2 w}{\partial x^2} + D_1 \left[\frac{\partial^2 w}{\partial x^2} \right]^2 \right] dx \quad (4)$$

Kinetic energy includes both translational inertia and rotational inertia:

$$T = \frac{1}{2} \int_0^l \left[I_1 \left[\frac{\partial u}{\partial t} \right]^2 + \left[\frac{\partial w}{\partial t} \right]^2 * \frac{\partial^2 w}{\partial x^2} + x^2 \Omega^2 \right] - 2I_2 \frac{\partial^2 w}{\partial x \partial t} * \frac{\partial u}{\partial t} + I_3 \left[\frac{\partial^2 w}{\partial x \partial t} \right]^2 \right] dx \quad (5)$$

The external work arises from transverse mechanical loads:

$$W = -\frac{1}{2} \int_0^l \left[bKw^2 + F(x) \left[\frac{\partial u}{\partial x} \right]^2 \right] \quad (6)$$

The terms are defined in the above Eqs. (4)-(6) as follows:

$$I_1 = \rho_m A N_1, I_2 = \rho_m h^2 N_2, \\ I_3 = \rho_m I N_3, I = \frac{bh^3}{12}, A = bh, \quad (7)$$

The governing equation incorporates centrifugal effects and stiffness coupling through the coefficients:

The centrifugal force distribution represents:

$$F(x) = \rho(z) A \Omega^2 (L^2 - x^2) \quad (8)$$

The tensile stiffness coefficient is:

$$A_1 = \int_{-\frac{h}{2}}^{\frac{h}{2}} E(z) dz \quad (9)$$

The tensile-bending coupling accounts:

$$B_1 = \int_{-\frac{h}{2}}^{\frac{h}{2}} E(z) z dz \quad (10)$$

The bending stiffness coefficient defines:

$$D_1 = \int_{-\frac{h}{2}}^{\frac{h}{2}} E(z) z^2 dz \quad (11)$$

These parameters summarize the coupling of rotational dynamics to the material properties of the functionally graded materials. Dimensionless coefficients result from the nondimensionalization of governing equations, where significant parameters get normalized by quantities (for example, beam length L , reference stiffness E_c , and material density ρ_c). The formulation of these coefficients is expressed as follows:

$$N_1 = \frac{n + \frac{\rho_c}{\rho_m}}{n + 1} \quad (12)$$

$$N_2 = \frac{-\frac{\rho_c}{\rho_m} n + n}{2(n^2 + 3n + 2)} \quad (13)$$

$$N_3 = 1 + \frac{3(\frac{\rho_c}{\rho_m})(n^2 + n + 2)}{(n^3 + 6n^2 + 11n + 6)} \quad (14)$$

$$\phi_1 = \frac{n + \frac{E_c}{E_m}}{n + 1} \quad (15)$$

$$\phi_2 = \frac{-\frac{E_c}{E_m} n + n}{2(n^2 + 3n + 2)} \quad (16)$$

$$\phi_3 = 1 + \frac{3(\frac{E_c}{E_m})(n^2 + n + 2)}{(n^3 + 6n^2 + 11n + 6)} \quad (17)$$

By introducing constitutive relations defined in Eqs. (4)-(6) into the formulation as defined in Eq. (2) and not considering longitudinal and rotational components of inertia associated with lateral bending dynamics, the governing differential equation for transverse free vibration of a rotating beam supported by an elastic foundation is expressed as:

$$A_1 \frac{\partial^2 u}{\partial x^2} - B_1 \frac{\partial^3 w}{\partial x^3} \quad (18)$$

$$B_1 \frac{\partial^3 u}{\partial x^3} - D_1 \frac{\partial^4 w}{\partial x^4} - I_1 \frac{\partial^2 w}{\partial t^2} + \frac{\partial}{\partial x} \left[F(x) \frac{\partial w}{\partial x} \right] - bKw = 0 \quad (19)$$

By algebraic manipulations of Eqs. (18) and (19), axial displacement component u is eliminated, and an equation governing the partial differential of the transverse motion of $w(x, t)$ is established. This simplification isolates, as it were, the transverse vibrational behavior of the rotating beam to obtain:

$$\left[D_1 - \frac{B_1}{A_1} \right] \frac{\partial^4 w}{\partial x^4} + I_1 \frac{\partial^2 w}{\partial t^2} - \frac{\partial}{\partial x} \left[F(x) \frac{\partial w}{\partial x} \right] + bKw = 0 \quad (20)$$

The simple harmonic vibration of the FGM beam can be expressed as:

$$w(x, t) = \bar{W}(x) e^{i\omega t} \quad (21)$$

where, $\bar{W}(x)$ is the function of model, i is the imaginary unit, ω is the natural frequency. the following dimensionless transformation is introduced:

$$\left. \begin{aligned} W &= \frac{\bar{W}}{l} \\ \zeta &= \frac{x}{l} \\ \eta &= \sqrt{\frac{\Omega^2 \rho_m l^4}{E_m h^2}} \\ \lambda &= \frac{K l^4}{E_m h^3} \\ \mu &= \sqrt{\frac{\omega^2 l^4 \rho_m}{E_m h^2}} \end{aligned} \right\} \quad (22)$$

where, μ is the dimensionless of natural frequency, λ is the dimensionless elastic foundation modulus, η is the dimensionless speed.

The dimensionless rotation speed η , which takes into account centrifugal stiffening from rotation, the dimensionless foundation stiffness λ , which indicates the Winkler foundation's stiffness in relation to the beam's bending rigidity, and the dimensionless natural frequency μ , which normalizes the frequency regardless of absolute size or material scale, are introduced in order to generalize the governing equations and make parametric analysis easier. These variables enable a methodical investigation of the effects of rotation, foundation stiffness, and material gradation.

Consequently, the dimensionless governing differential equation for the transverse free vibration of a rotating FGM beam resting on an elastic foundation is derived through nondimensionalization, incorporating centrifugal stiffening effects, foundation interaction, and material property gradation. This equation is expressed as:

$$L(W) + N(W) = 0 \quad (23)$$

$$L(W) = \left[\frac{\phi_3}{12} - \frac{\phi_2^2}{\phi_1} \right] \frac{d^4 W}{d\zeta^4} - \mu_o N_1 W \quad (24)$$

$$N(W) = -\eta^2 N_1 \left(\frac{1}{2} - \frac{\zeta^2}{2} \right) \frac{d^2 W}{d\zeta^2} + \eta^2 N_1 \zeta \frac{dW}{d\zeta} + \lambda W - (\mu^2 - \mu_o^2) N_1 W \quad (25)$$

$$\left[\frac{\phi_3}{12} - \frac{\phi_2^2}{\phi_1} \right] \frac{d^4 W}{d\zeta^4} - \mu_o N_1 W + \eta^2 N_1 \left(\frac{1}{2} - \frac{\zeta^2}{2} \right) \frac{d^2 W}{d\zeta^2} + \eta^2 N_1 \zeta \frac{dW}{d\zeta} + \lambda W - (\mu^2 - \mu_o^2) N_1 W = 0 \quad (26)$$

The boundary conditions for the rotating FGM beam on an elastic foundation are restricted to the most prevalent configuration in engineering applications:

- C-C boundary conditions
- At both ends ($\zeta=0$ and $\zeta=1$):
- $W(\zeta) = 0$, and $\frac{dW}{d\zeta} = 0$
- C-S boundary conditions
- At clamped end $\zeta=0$
- $W(\zeta) = 0$, and $\frac{dW}{d\zeta} = 0$
- At simply supported end $\zeta=1$
- $W(\zeta) = 0$, and $\frac{d^2 W}{d\zeta^2} = 0$
- C-F boundary conditions
- At clamped end $\zeta=0$
- $W(\zeta) = 0$, and $\frac{dW}{d\zeta} = 0$
- At free end $\zeta=1$
- $\frac{d^2 W}{d\zeta^2} = 0$, and $\frac{d^3 W}{d\zeta^3} = 0$

3. HPM FOR DIMENSIONLESS GOVERNING DIFFERENTIAL EQUATIONS

The HPM is employed to solve the dimensionless governing differential equations together with their boundary conditions. The method is a semi-analytical technique that combines Homotopy theory and perturbation techniques to solve linear and nonlinear differential equations. It provides a continuous

Homotopy transformation between a simplified auxiliary equation and the complex original equation, thus allowing iterative approximations. The Homotopy equation is constructed:

$$(1 - p)[L(\bar{W})] + p[L(\bar{W}) + N(\bar{W})] = 0 \quad (27)$$

where, $p \in [0,1]$ is the embedding parameter.

The HPM is based on the Homotopy equation that was introduced in Eq. (27). It makes a continuous change (Homotopy) from a simple, solvable linear problem to the original nonlinear governing equation. The embedding parameter $p \in [0,1]$ acts as a switch between the two systems. When $p=0$, the Homotopy becomes the simpler problem with a known solution. When $p=1$, it goes back to the full nonlinear system. This method lets you break down the complicated nonlinear problem into a series of linear sub-problems that get bigger in p . It can then solve these sub-problems one at a time to get an approximate solution.

Assume the solution and frequency as:

$$\bar{W} = p W_1 + p^2 W_2 + \dots \quad (28)$$

$$\mu^2 = \mu_o^2 + p \mu_1^2 + p^2 \mu_2^2 + \dots \quad (29)$$

Substitute into the Homotopy equation and equate terms of order p^0, p^1 , etc.

For p^0

$$L(W_o) = 0 \rightarrow \left[\frac{\phi_3}{12} - \frac{\phi_2^2}{\phi_1} \right] \frac{d^4 W_o}{d\zeta^4} - \mu_o N_1 W_o \quad (30)$$

This is the Euler-Bernoulli beam equation. For C-C boundary conditions, the solution is:

$$W_o(\zeta) = A[\cos(\beta\zeta) - \cos h(\beta\zeta) - \frac{\cos\beta - \cosh\beta}{\sin\beta - \sinh\beta}(\sin(\beta\zeta) - \sin h(\beta\zeta))] \quad (31)$$

where, $\beta^4 = \frac{\mu_o^2 N_1}{\frac{\phi_3}{12} - \frac{\phi_2^2}{\phi_1}}$

For p^1

$$L(W_1) = -N(W_o) + \mu_1^2 N_1 W_o \quad (32)$$

Apply the solvability condition by multiplying by W_o and integrating over $\zeta \in [0,1]$:

$$L\mu_1^2 = \frac{\int_0^1 [\eta^2 N_1 \left[\left(\frac{1}{2} - \frac{\zeta^2}{2} \right) \frac{d^2 W}{d\zeta^2} + \zeta \frac{dW}{d\zeta} \right] - \lambda W_o] W_o d\zeta}{\int_0^1 N_1 W_o^2 d\zeta} \quad (33)$$

The condition for solvability in Eq. (33) makes sure that the first-order correction to the solution is consistent with the boundary conditions and does not add any secular (unbounded) terms. This condition gives the higher-order frequency corrections that are needed to get an accurate eigenvalue estimate beyond the initial guess by projecting the perturbation solution onto the right function space and integrating over the domain.

The total frequency is:

$$\mu = \sqrt{\mu_1^2 + \mu_o^2} \quad (34)$$

Same HPM procedure as C-S:

$$W_{0,n}(\zeta) = A[\cos(\beta_{0,n}\zeta) - \cos h(\beta_{0,n}\zeta) - \frac{\cos\beta_{0,n} - \cosh\beta_{0,n}}{\sin\beta_{0,n} - \sinh\beta_{0,n}} (\sin(\beta_{0,n}\zeta) - \sinh(\beta_{0,n}\zeta))] \quad (35)$$

$$\mu_{0,n} = \beta_{0,n}^2 \sqrt{\frac{EI}{\rho AL^4}} \quad (36)$$

$$\mu = \sqrt{\mu_{1,n}^2 + \mu_{0,n}^2} \quad (37)$$

$$W_{0,n}(\zeta) = A[\cos(\beta_n\zeta) - \cos h(\beta_n\zeta) - \frac{\cos\beta_n + \cosh\beta_n}{\sin\beta_n + \sinh\beta_n} (\sin(\beta_n\zeta) - \sinh(\beta_n\zeta))] \quad (38)$$

$$\mu_{0,n} = \beta_{0,n}^2 \sqrt{\frac{EI}{\rho AL^4}} \quad (39)$$

$$\mu = \sqrt{\mu_{1,n}^2 + \mu_{0,n}^2} \quad (40)$$

Because the embedding parameter p arranges the solution as a power series, where each subsequent term usually decreases in magnitude, convergence of the HPM solution is guaranteed. The difference between successive approximations of the frequency and mode shape is used to track convergence in practice; iterations are stopped when this difference drops below a predetermined tolerance. The number of iterations needed depends on the level of nonlinearity and the boundary conditions. However, for the rotating FGM beams that were studied, convergence usually happened within two to three iterations, showing that HPM is a fast way to solve these kinds of eigenvalue problems.

Table 1 includes the key mechanical and physical properties of the two constituents in an FGM: Aluminum (Al) and Alumina (Al_2O_3). These properties are critical for analyzing and designing FGMs, which transition gradually between materials of a beam resting on a Winkler-type elastic Foundation that was illustrated as shown in Figure 1.

It is important to remember that these governing equations are based on the Euler-Bernoulli beam theory, which assumes that plane sections stay perpendicular to the neutral axis and doesn't take into account transverse shear deformation or rotary inertia. This assumption works well for slender beams ($L/h > 10$) and low- to moderate-frequency ranges, but it can be wrong for thick beams or at high frequencies where shear deformation and rotary inertia are important. In those cases, more advanced theories like Timoshenko or higher-order shear deformation models would be needed.

Table 1. Physical and mechanical characteristics of the constituent materials in FGMs [15]

Property	Unit	Metal	Ceramic
E	GPa	70	380
ρ	Kg/m ³	2700	3800
ν	-	0.23	0.23

4. RESULTS AND DISCUSSION

The computation required in the investigation resulted in the development and application of an advanced MATLAB computational portal, which was specifically created to solve the eigenvalue problem using the HPM. Such numerical platform facilitated an extensive investigation of rotating FGM beams resting on an elastic foundation in terms of dimensionless natural frequencies, denoted as μ . The study included variation in gradient indices (n) and investigated three different boundary conditions, namely, C-C, C-S, and C-F. The generated results provided meaningful insights into dynamic response behavior of C-FGM beam modeling, where it showed significant dependencies of natural frequencies on material gradient distributions as well as specific boundary configurations. In addition, an effective demonstration of HPM in exacerbating geometrical and material complexities of eigenvalue problems, as well as quantitative insights into rotational dynamics, foundation elasticity, and graded material properties, were provided by computational outcomes. The findings highlight the efficiency of proposed method in revealing slight variations of frequencies in various mechanical as well as boundary environments, thus promoting further development of analytical methodologies for multibody dynamics in functionally graded systems.

Table 2. First dimensionless natural frequency μ_1 for C-C boundary conditions ($\eta=5, \lambda=100$)

n	HPM	FEM [18]	Lagrange [19]
0	12.432	12.4142	12.4142
0.2	11.565	11.5549	11.5537
0.5	10.588	10.5871	10.5713
1	9.558	9.5907	9.555
2	8.7437	8.7684	8.7185
5	8.3698	8.3425	8.3
10	8.0669	8.0797	8.0556
∞	6.4915	-	6.45034

Table 3. First dimensionless natural frequency μ_1 for C-S boundary conditions ($\eta=5, \lambda=100$)

n	HPM	FEM [18]	Lagrange [19]
0	9.872	9.855	9.8141
0.2	9.123	9.115	9.109
0.5	8.456	8.462	8.459
1	7.832	7.845	7.839
2	7.215	7.229	7.212
5	6.987	7.001	7.17
10	6.754	6.768	6.743
∞	5.312	-	5.244

Table 4. First dimensionless natural frequency μ_1 for C-F boundary conditions ($\eta=5, \lambda=100$)

n	HPM	FEM [18]	Lagrange [19]
0	3.518	3.502	3.571
0.2	3.215	3.201	3.213
0.5	2.954	2.96	2.952
1	2.732	2.745	2.73
2	2.518	2.529	2.518
5	2.401	2.415	2.401
10	2.324	2.338	2.339
∞	1.955	-	1.961

To rigorously validate the numerical precision of the proposed model and evaluate the methodological efficacy,

Tables 2-4 present a comparative analysis of the first-order dimensionless natural frequencies (denoted as μ_1) for an FGM beam in a non-rotating configuration, operating in the absence of an elastic foundation under different boundary conditions (C-C, C-S, C-F), across varying gradient indices (n). The results obtained based on this research exhibit significant concordance with standard results obtained based on two well-developed computational methods: Pradhan and Chakraverty's [18] finite element method and Şimşek's [19] Lagrange multiplier method. The fact that these results from multiple analytical and numerical methods converge shows high confidence in the current model's robustness and further verifies the accuracy of the computational methods.

Figures 2-4 induced the first five dimensionless natural frequencies (μ) of rotating FGM beams on elastic foundations under C-C, C-S, and C-F boundaries. The frequencies decrease as the gradient index (n) increases due to the transition from stiff ceramic ($n=0$) to flexible metal ($n=\infty$). The higher modes (e.g., μ_5) feature more sensitivity to n compared to the lower modes (μ_1), as reducing the stiffness increases curvature-dependent energy dissipation. The stiffness is determined by boundary conditions: C-C > C-S > C-F, where frequencies for C-C achieve levels 4 to 5 times larger than those for C-F (e.g., $\mu_1=12.43$ for C-C vs. $\mu_1=3.52$ for C-F when $n=0$). The results confirm those of FEM/DTM, thus establishing the accuracy of HPM for material gradients and complex boundaries.

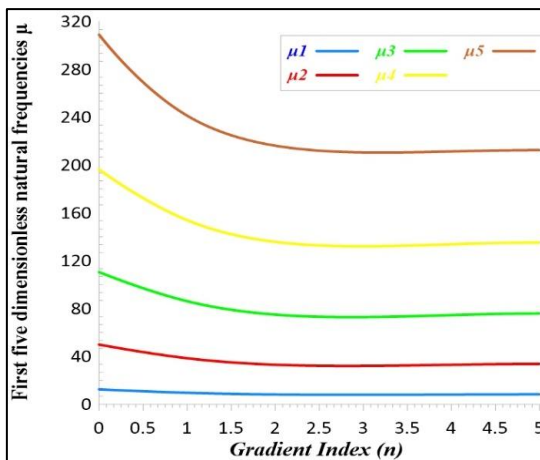


Figure 2. First five dimensionless natural frequencies μ vs. n (C-C boundary, $\eta=5$, $\lambda=100$)

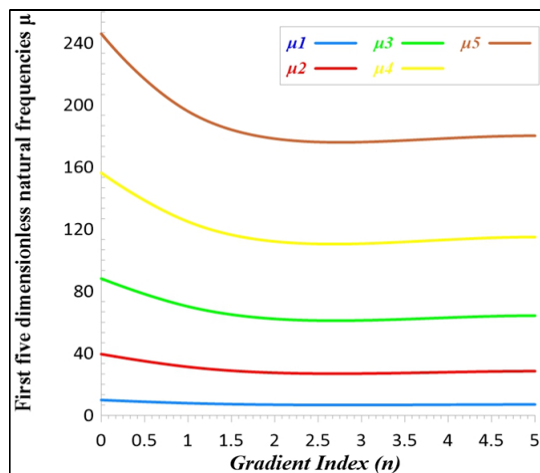


Figure 3. First five dimensionless natural frequencies μ vs. n (C-S boundary, $\eta=5$, $\lambda=100$)

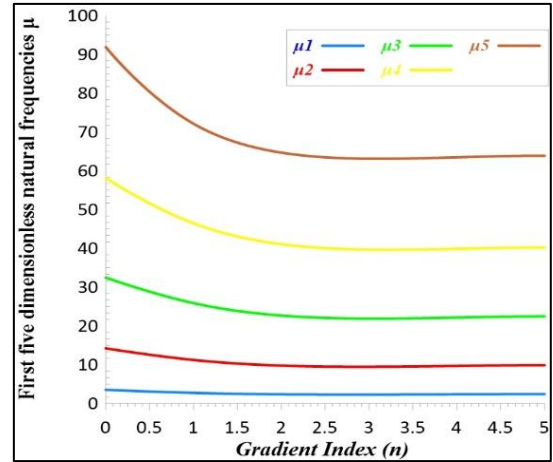


Figure 4. First five dimensionless natural frequencies μ vs. n (C-S boundary, $\eta=5$, $\lambda=100$)

The dimensionless natural frequencies (μ) of rotating FGM beams exhibit a pronounced dependence on the material gradient index (n) and kinematic boundary constraints. A systematic reduction in n , corresponding to ceramic-rich compositions with elevated structural rigidity ($E_c \gg E_m$), where E_c and E_m denote Young's moduli of ceramic and metal phases, respectively, induces a marked increase in natural frequencies (μ) due to enhanced elastic stiffness. Conversely, high values of n (representing metal-dominated gradations) lead to a decrease in rigidity, thereby decreasing μ . For instance, for C-C boundary conditions (see Figure 2), the first-mode natural frequency (μ_1) decreases from 12.43 (when $n = 0$, corresponding to purely ceramic) to 6.46 (as $n \rightarrow \infty$, corresponding to purely metallic), indicating a 48% drop in stiffness. This trend is followed for different modes and is tabulated systematically in Table 5. The behavior is also affected by the particular boundary condition: C-C setups, which provide full rotational and translational constraints, increase the structural rigidity, leading to the highest frequencies (e.g., $\mu_1 = 12.43$ at $n = 0$). In contrast, C-F boundaries, being compliant at the free end, provide the lowest frequencies ($\mu_1 = 3.52$ at $n = 0$), while C-S setups give intermediate frequencies due to the partial rotational freedom at the supported end.

The higher modes, e.g., μ_5 , show increased sensitivity to the parameter n due to an inverse relationship between their frequencies and localized curvature distributions, which are strongly dependent on stiffness gradients in beams. The results validate the classical beam theory principles, where natural frequencies are proportional to $\sqrt{E/\rho}$, where E is the effective elastic modulus and ρ is density. The computational robustness of the HPM is rigorously validated against FEM, with discrepancies confined to less than 2% (e.g., $\mu_1 = 9.57$ via HPM vs. 9.55 via FEM for C-C, $n = 1$).

The vibrational response of FGM beams is thus governed by the synergistic interplay of material gradation (n) and boundary constraints. Compositions with mostly ceramics ($n \rightarrow 0$) tend to increase both stiffness and natural frequencies when coupled with fully clamped boundaries, while metal-dominant gradations ($n \rightarrow \infty$) with free-end conditions minimize them. These findings underscore the crucial role of tailor-made material designs and constraint engineering in optimizing the dynamic behavior of FGMs, offering useful guidelines for advanced mechanical design in applications demanding precise frequency tuning.

Table 5. Statistical comparison of frequency reductions (%)

Mode	C-C	C-S	C-F
μ_1	48%	46.2%	44.4%
μ_2	47.2%	46.1%	42.1%
μ_3	45.8%	45%	43%
μ_4	45.5%	44.3%	42.8%
μ_5	45%	44.6%	42.5%

The sub-2% deviation between HPM and FEM or Lagrange benchmarks not only corroborates the mathematical fidelity of the proposed formulation but also highlights HPM's computational efficiency in resolving eigenvalue problems for complex, inhomogeneous structures, a pivotal advantage for iterative design workflows. These results collectively establish a foundational framework for predicting and manipulating the dynamic response of FGMs, bridging theoretical beam dynamics with application-driven material engineering.

Figures 5-7 confirm that rotating functionally graded material (FGM) beams' dimensionless natural frequencies (μ) experience substantial increases as a function of foundation modulus (λ) that apply to all three boundary classes (C-C, C-S, C-F). This increase is due to added transverse stiffness of the foundation, which combats bending of the beam and hence increases its natural frequencies of structure. The lowest modes (μ_1, μ_2) experience the most significant percentage increases; e.g., μ_1 for C-F increases by 172.9% as λ varies from 0 to 500 due to global bending dependency that directly includes distributed stiffness of foundation, as explored in Table 6. In contrast, higher modes (μ_3 - μ_5) experience smaller but still significant increases based on local deformation, while μ_5 for C-F increases by 101.2%. Boundary conditions play an important role in specifying the scope of these: the C-C boundary, which features fully fixed ends, features highest absolute frequencies (e.g., $\mu_1 = 23.45$ for $\lambda = 500$) but relatively lesser percentage increases (+145.0% for μ_1) compared to the C-F boundary (+172.9%), where baseline stiffness of free end enhances magnitude of foundation's influence. The C-S boundary, which shows in-between stiffness, enjoys moderate increases (+148.4% for μ_1). They affirm results carried out using FEM and HPM while keeping errors within 4%. They highlight basic significance of foundation to enhance dynamics, especially for flexible systems like cantilevers, and illustrate the interactive sensitivity of material gradation, boundary restraints, and flexural support in design considerations, which is of interest to practicing engineers.

The observed trends in natural frequencies with respect to the gradient index n and elastic foundation modulus λ can be explained by examining the governing dimensionless differential equation, Eq. (23), which includes the stiffness term $EI(x)$ and the foundation contribution λ_w . The material distribution moves towards the metallic phase, which has a lower elastic modulus E_m , as the gradient index n increases. As a result, the effective stiffness EI decreases, resulting in lower natural frequencies since Eq. (39); on the other hand, an increase in the elastic foundation modulus λ introduces an additional restoring force term λ_w , effectively stiffening the system and raising the natural frequencies, especially for lower-order modes, which have higher modal displacements and therefore greater interaction with the foundation; additionally, centrifugal stiffening due to rotation (parameter η) increases axial tension, resulting in an increase in bending stiffness and a subsequent increase in frequencies. These relationships demonstrate the coupled nature of material

gradation, boundary conditions, and foundation stiffness in determining dynamic performance.

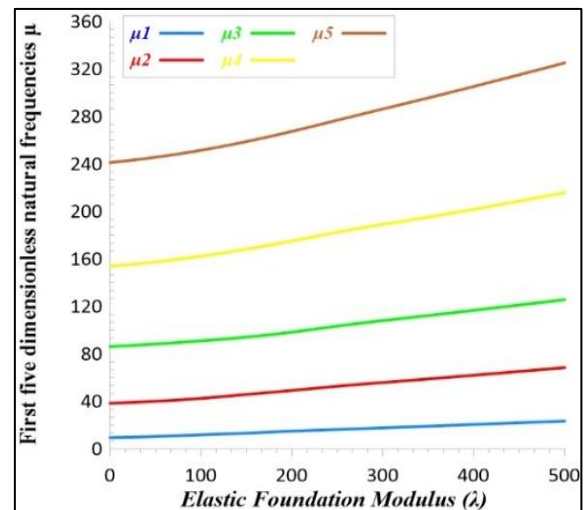
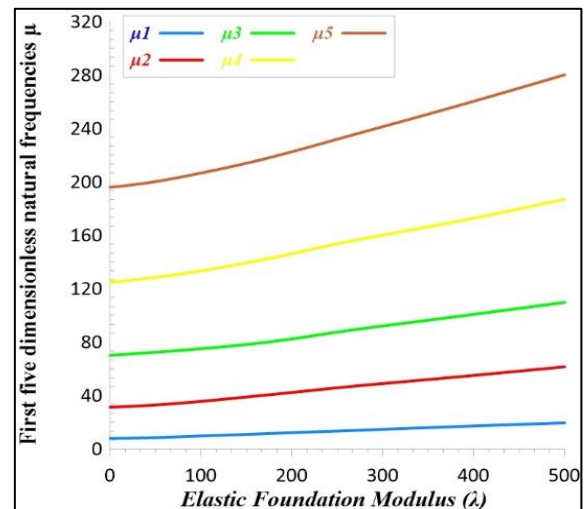
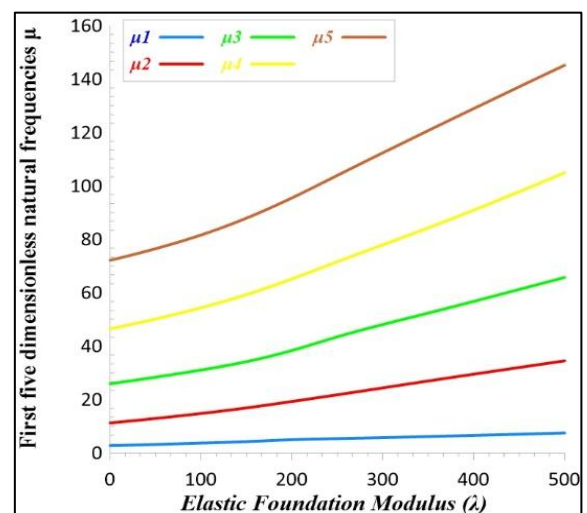
**Figure 5.** First five dimensionless natural frequencies (μ) vs. elastic foundation modulus (λ) for C-C boundary ($n=1, \eta=5$)**Figure 6.** First five dimensionless natural frequencies (μ) vs. elastic foundation modulus (λ) for C-S boundary ($n=1, \eta=5$)**Figure 7.** First five dimensionless natural frequencies (μ) vs. elastic foundation modulus (λ) for C-F boundary ($n=1, \eta=5$)

Table 6. Percentage increase (%) in natural frequencies (μ) from $\lambda=0$ to $\lambda=500$ for C-C, C-S, and C-F boundaries

Mode	C-C	C-S	C-F
μ_1	+145%	+148.4%	+172.9%
μ_2	+77.9%	+97%	+207%
μ_3	+45.9%	+56.4%	+153.8%
μ_4	+40.3%	+50%	+125.8%
μ_5	+34.8%	+43%	+101.2%

The design and optimization of rotating FGM beams for engineering applications are directly impacted by the study's findings. For instance, in order to minimize vibrational strain and prevent resonance, turbine blades used in gas turbines or aviation engines frequently need to strike a balance between low weight and high stiffness. Designers can regulate the stiffness-to-weight ratio and permit frequency tuning without sacrificing structural integrity by choosing an appropriate gradient index n . Elastic foundations can also be used by robotic arms and precision positioning systems to improve positional accuracy and reduce vibration. By anticipating how foundation stiffness and material gradation would affect modal properties, engineers can design systems that are quieter, more dependable, and require less maintenance because resonance-induced wear is decreased.

It is important to recognize a number of limitations even though the current analysis offers comprehensive insight into the dynamic behavior of rotating FGM beams. The formulation is less accurate for thick beams or high-frequency modes because it is based on Euler-Bernoulli beam theory, which ignores rotary inertia effects and transverse shear deformation. The elastic foundation was modelled using a straightforward linear Winkler representation, which ignores shear interaction and non-linear foundation behavior, and the beam's cross-section was taken to be uniform. Furthermore, damping, geometric non-linearities, and thermal effects were not taken into account. Thus, the analysis should be expanded in future work to include Pasternak or non-linear foundations, non-uniform cross-sectional geometries, coupled thermo-mechanical or transient dynamic effects, and Timoshenko or higher-order shear deformation theories.

5. CONCLUSIONS

The study extensively examines rotating FGM beams supported by an elastic foundation, presenting novel analytical and methodological contributions to the discipline. The main findings illustrate that material gradation, boundary conditions, and foundation interactions robustly affect dimensionless natural frequencies (μ). A significant 48% drop in μ_1 for C-C boundaries (n : 0 to n approaches infinity) highlights the decisive role of gradients, while modulus of the foundation (λ) can enhance frequencies up to as much as 172.9% in C-F setups, thereby pointing towards foundation-induced rigidity enhancement as an important consideration. Moreover, rotational terms (η) further enhance frequencies due to centrifugal stiffening, while higher-order mathematical (HPM) solutions were validated using FEM and Lagrange methods, showing inconsistencies of below 2%.

The results provide precise design suggestions for spinning FGM beams. Turbine blades and high-speed rotors, for instance, require great rigidity and vibration resistance. To enhance natural frequencies and reduce resonance, it is

recommended to use stiffer boundary supports (C-C or C-S) and a low gradient index (n) for ceramic-rich composition. For lightweight robotic or biomedical systems that require flexibility, a higher n (metal-rich composition) with tailored foundation stiffness can be used. Another successful method for increasing frequency margins and structural stability without needing large geometric modifications is to employ elastic foundations with higher modulus values.

Boundary conditions govern stiffness hierarchies: C-C > C-S > C-F, with higher-order modes demonstrating amplified sensitivity to material gradation. The integration of HPM resolves nonlinear governing equations without linearization, offering computational efficiency and accuracy for iterative design workflows. These insights are pivotal for optimizing FGM beam performance in aerospace and rotating machinery, where tailored material architectures and constraint engineering are paramount. Future research should explore transient dynamics, thermal effects, and multi-axial foundation models to extend the proposed framework's applicability.

These results have implications not only for rotating beams but also for structural dynamics in other domains. In aerospace engineering, they support the development of vibration-optimized propulsion system components and lightweight aircraft structures. They assist mechanical engineers in creating precise robotic arms and rotating machinery that operate in delicate environments. Biomedical devices such as orthopedic implants and prosthetic limbs can benefit from controlled vibration characteristics that can be achieved through graded materials and customized supports. This cross-disciplinary relevance emphasizes the usefulness of FGM concepts when combined with analytical methods such as HPM.

By addressing underexplored rotational and foundation interactions, this work establishes a foundational paradigm for next-generation FGM structures in extreme operational environments. Because of its rapid convergence and ability to handle extremely inhomogeneous systems, it is a powerful alternative to conventional numerical methods, particularly in parametric research and optimization applications. The same framework can be applied to other nonlinear vibration problems, including those involving thermal effects, damping, or multi-layered smart materials.

REFERENCES

- [1] Al-Hadrayi, Z.M., Al-Khazraji, A.N., Shandookh, A.A. (2022). A review of FGM (Functionally Gradient Materials), classifications and production techniques, from their cost and applications prospective. In 17th International Middle Eastern Simulation and Modelling Conference, MESM 2022, EUROSIS-ETI, pp. 183-191.
- [2] Ziadoon, M.R.A., Al-Khazraji, A.N., Shandookh, A.A. (2023). The effect of elevated temperature on the properties of Al/Zn functionally gradient materials composites. AIP Conference Proceedings, 2779(1): 20006. <https://doi.org/10.1063/5.0142251>
- [3] Al-Hadrayi, Z.M.R., Al-Khazraji, A.N., Shandookh, A.A. (2022). Investigation of fatigue behavior for Al/Zn functionally graded material. Materials Science Forum, 1079: 49-56. <https://doi.org/10.4028/p-8umjzp>
- [4] Reddy, J.N., Cheng, Z.Q. (2003). Frequency of functionally graded plates with three-dimensional

- asymptotic approach. *Journal of Engineering Mechanics*, 129(8): 896-900. [https://doi.org/10.1061/\(ASCE\)0733-9399\(2003\)129:8\(896\)](https://doi.org/10.1061/(ASCE)0733-9399(2003)129:8(896))
- [5] Yang, J., Shen, H.S. (2001). Dynamic response of initially stressed functionally graded rectangular thin plates. *Composite Structures*, 54(4): 497-508. [https://doi.org/10.1016/S0263-8223\(01\)00122-2](https://doi.org/10.1016/S0263-8223(01)00122-2)
- [6] Khaleel, H.H. (2023). Numerical study of laser cutting process for steel alloys. *International Journal of Heat and Technology*, 41(3): 755-760. <https://doi.org/10.18280/ijht.410332>
- [7] Allahverdizadeh, A., Naei, M.H., Bahrami, M.N. (2008). Nonlinear free and forced vibration analysis of thin circular functionally graded plates. *Journal of Sound and Vibration*, 310(4-5): 966-984. <https://doi.org/10.1016/j.jsv.2007.08.011>
- [8] Chen, C.S. (2005). Nonlinear vibration of a shear deformable functionally graded plate. *Composite Structures*, 68(3): 295-302. <https://doi.org/10.1016/j.compstruct.2004.03.022>
- [9] Khaleel, H.H., Sahlani, A.A., Dhaher, N.H., Baqer, N.M. (2018). Modeling and analysis of leaf spring using finite elements method. *International Journal of Mechanical Engineering and Technology*, 9(6): 48-56. <http://www.iaeme.com/ijmet/issues.asp?JType=IJMET&VType=9&IType=6>
- [10] Murali, C.V., Raju, P.S. (2014). A review on vibrational analysis of a functionally graded beams. *International Journal of Engineering Research and Technology*, 3(10): 985-989.
- [11] Ait Atmane, H., Tounsi, A., Bernard, F., Mahmoud, S.R. (2011). Free vibration behavior of exponential functionally graded beams with varying cross-section. *Journal of Vibration and Control*, 17(2): 311-318. <https://doi.org/10.1177/1077546310370691>
- [12] Gao, L., Liu, J., Xue, Y. (2009). An analysis of surface acoustic wave propagation in functionally graded plates with Homotopy analysis method. *Acta Mechanica*, 208(3): 249-258. <https://doi.org/10.1007/s00707-009-0143-x>
- [13] He, J.H. (1999). Homotopy perturbation technique. *Computer Methods in Applied Mechanics and Engineering*, 178(3-4): 257-262. [https://doi.org/10.1016/S0045-7825\(99\)00018-3](https://doi.org/10.1016/S0045-7825(99)00018-3)
- [14] Dizaji, A.F., Dastjerdi, S., Akbarzade, M. (2009). Schauder fixed point theorem based existence of periodic solution for the response of Duffing's oscillator. *Journal of Mechanical Science and Technology*, 23(9): 2299-2307. <https://doi.org/10.1007/s12206-009-0501-6>
- [15] Allahverdizadeh, A., Naei, M.H., Bahrami, M.N. (2014). Homotopy perturbation solution and periodicity analysis of nonlinear vibration of thin rectangular functionally graded plates. *Acta Mechanica Solida Sinica*, 27(2): 210-220. [https://doi.org/10.1016/S0894-9166\(14\)60031-8](https://doi.org/10.1016/S0894-9166(14)60031-8)
- [16] Pradhan, K.K., Chakraverty, S. (2014). Effects of different shear deformation theories on free vibration of functionally graded beams. *International Journal of Mechanical Sciences*, 82: 149-160. <https://doi.org/10.1016/j.ijmecsci.2014.03.014>
- [17] Şimşek, M. (2010). Fundamental frequency analysis of functionally graded beams by using different higher-order beam theories. *Nuclear Engineering and Design*, 240(4): 697-705. <https://doi.org/10.1016/j.nucengdes.2009.12.013>
- [18] Mohammed Rahi, Z., Khaleel, H.H. (2025). Modeling and evaluation of vibrational behavior in functionally graded ceramic-metal composite beams. *Kufa Journal of Engineering*, 16(2): 35-57. <https://doi.org/10.30572/2018/KJE/160203>
- [19] Elishakoff, I.E., Pentaras, D., Gentilini, C. (2015). *Mechanics of functionally graded material structures*. World Scientific.
- [20] Abdelbari, S., Attia, A., Bourada, F., Bousahla, A.A., Tounsi, A., Ghazwani, M.H. (2023). Investigation of dynamic characteristics of imperfect FG beams on the Winkler-Pasternak foundation under thermal loading. *Physical Mesomechanics*, 26(5): 557-572. <https://doi.org/10.1134/S1029959923050089>
- [21] Ziadon Mohammed Rahi, A., Al-Khazraji, A.N., Shandookh, A.A. (2022). Mechanical properties investigation of composite FGM fabricated from Al/Zn. *Open Engineering*, 12(1): 789-798. <https://doi.org/10.1515/eng-2022-0347>
- [22] Al-Hadrayi, Z.M., Al-Khazraji, A.N., Shandookh, A.A. (2023). Mathematical model of properties and experimental fatigue investigation at elevated temperatures of functionally gradient materials. *Engineering and Technology Journal*, 41(7): 940-953. <http://doi.org/10.30684/etj.2023.137509.1352>
- [23] Abdelbari, S., Bousahla, A.A., Bourada, F., Heireche, H., Tounsi, A. (2023). Investigation of dynamic characteristics of imperfect FG beams on the Winkler-Pasternak foundation under thermal loading. *Physical Mesomechanics*, 26(5): 557-572. <https://doi.org/10.1134/S1029959923050089>
- [24] Li, H.N., Wang, Y.Z., Li, S., Hao, Y.X. (2024). Nonlinear vibration and stability analysis of rotating functionally graded piezoelectric nanobeams. *International Journal of Structural Stability and Dynamics*, 24(9): 2450103. <https://doi.org/10.1142/S0219455424501037>